

# Advancing Time Series Wildfire Spread Prediction: Modeling Improvements and the WSTS+ Benchmark

Saad Lahrichi

University of Missouri  
Columbia, MO 65201

saad.lahrichi@missouri.edu

Jake Bova

University of Montana  
Missoula, MT 59802

jacob.bova@umont.edu

Jesse Johnson

University of Montana  
Missoula, MT 59802

jesse.johnson@umont.edu

Jordan Malof

University of Missouri  
Columbia, MO 65201

jmdrp@missouri.edu

## Abstract

Recent research has demonstrated the potential of deep neural networks (DNNs) to accurately predict wildfire spread on a given day based upon high-dimensional explanatory data from a single preceding day, or from a time series of  $T$  preceding days. Here, we introduce a variety of modeling improvements that achieve state-of-the-art (SOTA) accuracy for both single-day and multi-day input scenarios, as evaluated on a large public benchmark for next-day wildfire spread, termed the *WildfireSpreadTS* (WSTS) benchmark. Consistent with prior work, we found that models using time-series input obtained the best overall accuracy. Furthermore, we create a new benchmark, *WSTS+*, by incorporating four additional years of historical wildfire data into the WSTS benchmark. Our benchmark doubles the number of unique years of historical data, expands its geographic scope, and, to our knowledge, represents the largest public benchmark for time-series-based wildfire spread prediction.

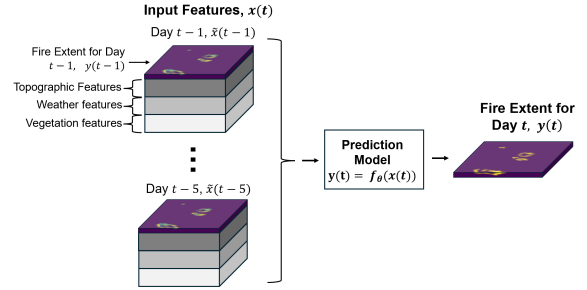


Figure 1. The wildfire prediction models take as input a geospatial raster of several variables: vegetation, topography, and weather features, alongside the current day fire mask. We consider two prediction scenarios: one in which the model receives input features from only one preceding day, denoted  $t-1$ , and another in which we provide the model five previous days of features as input. In either case, the model must predict a binary mask indicating the extent of the fire on day  $t$ .

## 1. Introduction

Wildfires are a global cause of concern that have severe human, economical, and environmental impacts, with the average annual economic burden from wildfires falling between \$71.1 billion and \$347.8 billion [38]. Due to climate change, many regions are getting hotter and drier, which lengthens wildfire seasons and exacerbates their effect. In order to better manage, mitigate, and prevent wildfires, accurately predicting their spread is essential. In this work, we focus on the problem of next-day wildfire spread prediction, where we are provided with current and/or histori-

cal information about a particular wildfire, and then tasked with predicting its spatial extent on the following day.

A variety of approaches have been investigated to solve this problem, such as those based upon machine learning models [4, 8, 22], or physics-based and observationally-informed models [1, 10, 11]. In this work, however, we focus on a promising emerging class of techniques that utilize high-capacity machine learning models – namely deep neural networks (DNNs) – to predict wildfire spread using high-dimensional explanatory input data. These input data typically comprise a geospatial map of the current extent of the fire, as well as maps of explanatory features such as topography, climate, weather, and vegetation indices. Based upon these input data, the model is tasked with producing

a geospatial map, or an image, reflecting the spatial extent of the fire on the following day, i.e. the spread of fire into regions that have not burned, and the extinction of fire in regions that have ceased burning. See Fig. 1 for an illustration.

DNN-based models have achieved impressive prediction accuracy, and have garnered substantial attention in recent years for wildfire modeling, including specifically next-day wildfire prediction. A variety of DNN-based models have been proposed to solve next-day prediction, including convolutional models [5, 28, 30], attention-based models such as transformers [37], and spatio-temporal models [3, 31]. Most existing research has focused on next-day prediction where only explanatory data from the current day is provided (day  $t$  only, in Fig. 1). However, recent research found that models utilizing a time-series of  $T$  days of historical data can achieve greater prediction accuracy [15], suggesting this as an important new direction in next-day wildfire prediction.

**Contributions of this Work** In this work, we introduce a variety of modeling improvements to both the single-day ( $T = 1$ ) and time-series ( $T > 1$ ) input scenarios. Our results show that these improvements lead to substantial increases in accuracy over the existing state-of-the-art, as demonstrated on the WildfireSpreadTS (WSTS) benchmark [15], an extension of the well-studied Next Day Wildfire Spread benchmark [20] to support time-series prediction. We chose WSTS because it is the only publicly available benchmark for time-series wildfire prediction, and employs a rigorous and realistic 12-fold leave-one-year-out cross-validation. Our best model achieves a new SOTA on the WSTS benchmark by a large margin. Lastly, we introduce WSTS+, an extended benchmark for next-day wildfire spread, constructed by doubling the number of years of historical wildfire events in WSTS. The WSTS+ benchmark reveals an important emerging challenge in wildfire modeling: data heterogeneity. We summarize our contributions as follows:

- *SOTA Single-Day ( $T = 1$ ) Prediction.* We introduce a variety of improvements to modeling single-day wildfire prediction, leading to 37% improvement in performance over existing models.
- *SOTA Time-Series ( $T > 1$ ) Prediction.* We introduce a variety of modeling improvements, resulting in a 28% performance improvement in accuracy over existing models. We also find that our time-series models outperform single-day models, resulting in a new overall SOTA on wildfire prediction.
- *WSTS+: An expanded Public Benchmark for Next-Day Wildfire Modeling.* Our proposed benchmark includes twice the years of historical data as its predecessor, WSTS, resulting, to our knowledge, in the largest public

benchmark for *time-series* next-day wildfire spread prediction. It also reveals an emerging challenge for the wildfire modeling community: data heterogeneity.

The rest of the paper is structured as follows: we formulate our problem setting in Sec. 2, Sec. 3 reviews related works, Sec. 4 describes our adopted benchmark, we present some preliminaries in Sec. 5, Sec. 6 details our experimental setting and results, Sec. 7 introduces our expanded benchmark, and Sec. 8 summarizes our findings.

## 2. Problem Setting

In its general formulation, the goal of next-day wildfire spread prediction is to predict a wildfire’s spatial extent on some  $t^{th}$  day, denoted  $y(t)$ , given explanatory data from one or more *preceding* days, denoted  $x(t)$ . We adopt the more specific settings of recent literature [15, 20], as illustrated in Fig. 1, which assume there are  $T$  consecutive previous days of explanatory data, so that  $x(t) = \{\tilde{x}(t - i)\}_{i=1}^T$ , and each  $\tilde{x}(t)$  comprises a geospatial raster, so that  $\tilde{x}(t) \in \mathbb{R}^{H \times W \times C}$ , where  $H, W$  correspond to spatial dimensions, and  $C$  represents the number of explanatory variables, which may include previous fire masks (e.g.,  $y(t) \subset \tilde{x}(t)$ ). The fire extent is encoded in a binary geospatial image,  $y(t) \in \{0, 1\}^{H \times W}$ , where a value of one indicates the presence of a fire. Our goal is then to use a dataset of historical wildfire data to infer parameters,  $\theta$  of a predictive model of the form  $y(t) = f_{\theta}(x(t))$ .

## 3. Related Works

**Next Day Wildfire Segmentation** To apply DNNs to fire spread prediction, recent research has framed the spread problem as a semantic segmentation one, and developed multiple datasets to support this framing. [20] created Next-Day Wildfire Spread, a dataset for mono-temporal fire spread prediction. They developed a custom convolutional autoencoder that takes as input various explanatory variables and outputs a binary mask indicating fire presence at each pixel. Similarly, [15] extended the dataset to include multi-temporal prediction, added more explanatory variables, and higher resolution fire masks. They achieved the best performance using a standard Unet model and a Unet model with temporal attention (UTAE) [14]. Other datasets aim to predict beyond next-day and forecast fire behavior several days in advance, e.g., [34] developed SeasFire Cube and trained Unet++ models [41] for medium-term fire prediction, between 8 and 64 days. [23] improved upon the collected data cube and found that the LSTM and ConvLSTM models outperformed the Fire Weather Index (FWI). In FireSight, [18] collected a dataset using remote sensing data from 20 datasets, and trained a 3D UNet model to model short-term fire hazard, between 3 and 8 days.

**Other Approaches** Aside from segmentation, other formulations have been developed for modeling fire spread using deep learning (DL). [36] used a CNN-based Reinforcement Learning model that predicts the best action as burn or no burn given current conditions. [16] developed a probabilistic cellular automata model to simulate wildfire spread. In [26], the authors developed Sim2Real-Fire, a synthetic, high-resolution dataset for fire spread forecast and backtracking and outperformed the considered baselines using a custom Transformer model. We refer the readers to [40] for a more comprehensive review of DL for wildfire prediction.

**Next Day Wildfire Prediction with Time-Series** In contrast to most existing work (e.g., [12, 24, 37, 39]), we focus on utilizing a time-series of features for next-day wildfire spread prediction, which has been cited as an important emerging area of research [12, 15, 24]. Historically, time-series modeling has been challenging due to the lack of appropriate public datasets to train and evaluate models for this task. Recently, [15], building upon the work of [20], developed the first multi-temporal dataset for time-series prediction. Notably, they found that models using a time-series of input tend to outperform those using a single day, reinforcing the importance of this research direction.

## 4. The WSTS Benchmark

In this work, we employ the WildfireSpreadTS benchmark [15]. The dataset includes 607 wildfire events across the western United States between 2018 and 2021, totaling 13,607 daily multi-channel images. These 23 channels include data on active fires, weather, topography, and vegetation, resampled to a common resolution of 375 meters, providing a multi-modal and multi-temporal framework for modeling fire spread. A key feature of this benchmark is a rigorous 12-fold cross-validation evaluation procedure. Each fold of the cross-validation includes all wildfire events from a single year, so that the trained models are always evaluated on wildfire events from a previously unseen year, reflecting real-world use of wildfire prediction models.

## 5. Preliminaries

**U-Net [35]** The U-Net is a widely-used architecture for segmentation, including for remote sensing applications [25]. There are now many variations of the U-Net, including modern variants that utilize attention (e.g., SwinUnet [6]). The U-Net typically includes three distinguishing architectural features: an encoder,  $f_{\theta_{En}}$  with parameters  $\theta_{En}$ ; a decoder,  $f_{\theta_{De}}$  with parameters  $\theta_{De}$ ; and skip connections between the encoder and decoder, as is illustrated in Fig. 2. The original U-Net in [35] employed an encoder with relatively few layers that were trained from scratch. It has

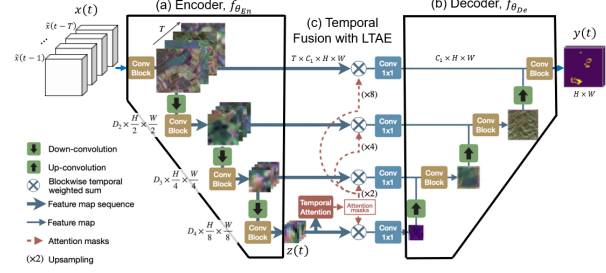


Figure 2. Illustration of the U-Net and UTAE models, adapted from [14] to our wildfire problem. The U-Net consists of (a) an encoder and (b) a decoder, with skip connections connecting intermediate layers. For a U-Net we have  $T = 1$  and temporal fusion, part (c), would not be present. The UTAE is similar to the U-Net except  $T > 1$  and it includes Temporal Fusion, specifically with an LTAE.

been found, however, that utilizing larger pre-trained encoders (e.g., ResNet models [19]) can be beneficial, including specifically when applied to remote sensing data[21].

**UTAE [14]** The UTAE was originally developed for satellite imagery, and is essentially a U-Net that has been modified to process a time-series of imagery. The UTAE encodes each entry in the time-series independently using a shared encoder, and then fuses the resulting embeddings from each day using a Lightweight Temporal Self-Attention (LTAE) block [13]. This process is illustrated in Fig. 2 in the context of our wildfire spread problem. Given a  $T$ -length time-series of input, the encoder produces a series of  $T$  embeddings  $z(t) = \{\tilde{z}(t - i)\}_{i=1}^T$  where  $\tilde{z}(t) \in \mathbb{R}^{D_4 \times \frac{H}{8} \times \frac{W}{8}}$  at the output of the last layer of the encoder, as illustrated in Fig. 2. Then the LTAE computes an attention mask,  $a \in \mathbb{R}^{T \times \frac{H}{8} \times \frac{W}{8}}$ , which is utilized to combine the  $T$  embeddings. Before computing the temporal attention, LTAE adds a sinusoidal positional embedding,  $p(\tilde{t})$  to each input embedding, where  $\tilde{t} \in [1, 365]$  is an integer representing the day of the year, and  $p(\tilde{t})$  maps  $\tilde{t}$  to a unique sinusoidal representation. This positional embedding is motivated by the original application of UTAE to agricultural segmentation, where the appropriate segmentation depends heavily upon the day of the year. Once the attention mask is computed, it is then upsampled, and applied to the encoder embeddings output at each resolution to collapse the temporal dimension. After all temporal dimensions are collapsed, a conventional U-Net-like decoder is applied to the collapsed embeddings.

## 6. Improving Wildfire Spread Prediction

In this section, we describe our methods for  $T = 1$  and  $T = 5$  scenarios, respectively, as well as experiments to support them (e.g., ablations). Results for our developed

benchmark models are reported in Tab. 2, in terms of Average Precision (AP) using 12-fold leave-one-year-out cross-validation on the WSTS benchmark, following prior work [15]. Also following [15], we report model performance for three feature sets: vegetation features only (Veg), a combination of vegetation and topographic features (Multi), and all features (All), which includes additional weather forecast features. Full experimental details are provided in the supplemental information. Models in Tab. 2 with citations correspond to the three current best models on WSTS, as reported in [15]. All other models reported in Tab. 2 were developed in this work.

### 6.1. Single-Day Input ( $T = 1$ )

The current  $T = 1$  SOTA utilizes a U-Net architecture with a ResNet-18 encoder, and is denoted Res18-Unet[15]. Therefore we focus our investigation on improving the Res18-Unet[15].

**Modeling Improvements** We next describe our improvements to the Res18-Unet[15] at a high level. More details can be found in the supplement.

(i) *Improved Encoders.* We hypothesize that better performance may be obtained with larger encoders, or those that utilize attention mechanisms. Recent studies have indicated attention-based models to be superior to convolutional models for wildfire spread [24, 37, 39, 42], although these studies did not utilize the rigorous 12-fold leave-one-year out cross-validation in the WSTS benchmark that we use here. Therefore we investigate the use of a ResNet50 [19] encoder, as well as the attention-based SwinUnet-Tiny encoder [6].

(ii) *Utilizing Pre-trained Parameters.* Utilizing pre-trained weights to initialize training is a well-established technique to improve model accuracy in data-limited scenarios, such as the WSTS benchmark. We introduce pre-trained weights into each of the encoders that we consider (i.e., ResNet18, ResNet50, and SwinUnet), while the decoders are trained from scratch.

(iii) *Improved Loss Functions.* The existing SOTA Res18-Unet [15] is trained using weighted binary cross-entropy loss. However, it has been established that Jaccard/Dice losses are often superior alternatives for segmentation tasks [9], and focal loss has been shown effective for class imbalance [27] (the WSTS benchmark exhibits severe class imbalance), and for wildfire spread in particular [12]. Therefore we investigate and compare the aforementioned losses in our experiments.

(iv) *Improved Hyperparameter Optimization.* The existing SOTA Res18-Unet [15] was trained by selecting the model with the highest F1 score on the validation, however, all models on WSTS are evaluated utilizing the average precision (AP) metric [15]. We investigate aligning the valida-

tion and testing metrics by using AP for both.

For our experiments, we consider a U-Net with a ResNet-18 encoder (denoted *Res18-Unet*), and a ResNet-50 encoder (denoted *Res50-Unet*), and a SwinUnet-Tiny (denoted *SwinUnet*). For each of these models, we perform a grid search over all combinations of learning rates ( $[1e-1, 1e-2, 1e-3, 1e-4, 1e-5]$ ), loss functions (BCE, Focal, Dice, Jaccard), and the use of pre-training or not (a binary choice). Following [15], we use a single fold of the 12-fold cross-validation, and only one of the three feature sets (the "All" set) for this optimization. As discussed, in contrast to previous work, we utilize AP during validation to select the best models instead of F1. The focal loss has two hyperparameters:  $\alpha$ , set as the inverse frequency of positive class pixels, and  $\gamma$ , set to its default value of two.

**Experimental Results** We found that pre-training was nearly always beneficial, and that Focal Loss usually yielded substantial improvements compared to our other candidate losses. Therefore, for the WSTS benchmark, we included both pre-training and focal loss in all three of our models: *Res18-Unet*, *Res50-Unet*, and *SwinUnet*. As an ablation study, Tab. 1 reports the performance of our *Res18-Unet* on the full WSTS benchmark, where we progressively remove each of our improvements to assess its impact. Our results indicate that each improvement is highly beneficial, or at least not significantly harmful.

Tab. 2 reports the performance of our three models on the WSTS benchmark, compared to the best existing  $T = 1$  model, *Res18-Unet*[15]. Our *Res18-Unet* is identical to the *Res18-Unet*[15], except for our aforementioned modifications, and obtains substantially higher AP across all candidate input features considered: a 37% improvement on average.

Our other two models, *Res50-Unet* and *SwinUnet*, also substantially outperform the existing *Res18-Unet*[15]. However, despite having approximately twice the number of trainable model parameters of *Res18-Unet*, we find that our model outperforms the two larger models in most cases. *Our Res18-Unet also obtains the highest overall AP (0.468) for the  $T = 1$  models when utilizing the "Multi" feature set, establishing a new SOTA on WSTS for  $T = 1$ .*

Several recent studies have reported that large and/or attention-based models achieve SOTA accuracy for  $T = 1$  wildfire spread prediction [24, 37, 39, 42]. However, we find here that with simple improvements and appropriate optimization, *Res18-Unet* outperforms such models. We also suspect that the more rigorous (and potentially more real-world) leave-one-year-out cross-validation adopted by the WSTS benchmark may penalize more complex models for overfitting, compared to the *Res18-Unet*.

In Fig. 3, we qualitatively evaluate our *Res18-Unet* and *Res50-Unet* against the Res18-Unet [15]. Each row cor-



Table 1. Ablation showing the impact of the successive removal of each of our improvements on a *Res18-Unet* trained on Vegetation features

Model	Test AP	Percent Decrease
Res18-Unet (ours)	$0.455 \pm 0.092$	—
No pretraining	$0.456 \pm 0.086$	−0.22
No focal loss	$0.345 \pm 0.084$	24.18
No AP as validation	$0.321 \pm 0.078$	29.45

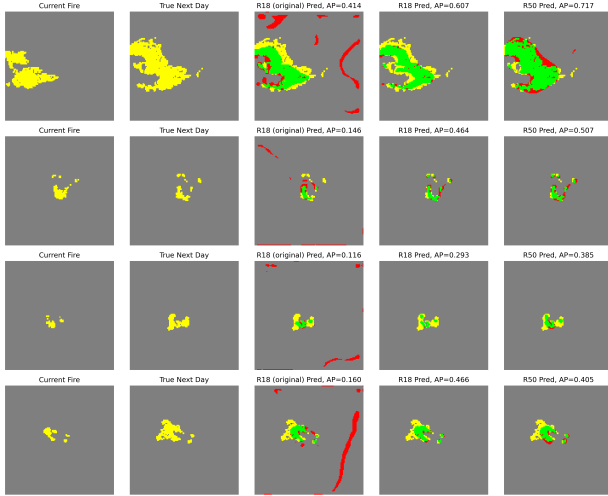


Figure 3. Sample predictions made by the Res18-Unet [15], our *Res18-Unet*, and *Res50-Unet*. The two leftmost columns show the current fire spread  $y(t-1)$  and the next-day label  $y(t)$ . True positive pixels are colored in green, while false positives are colored in red

responds to a fire event and the columns show the current fire, the next day label, and the predictions of each model. Yellow represents the fire extent, green shows correctly predicted burned areas, and red shows false positives. We observe that the original model tends to overpredict fire spread, leading to multiple red patches where no fire actually occurs. However, the model also underpredicts in areas where the fire spreads, capturing some, but not the full extent of the fire. On the other hand, we observe that our models make consistently more accurate predictions, with far fewer false positives, and slightly better matching green areas.

## 6.2. Time-Series Input, $T = 5$

Existing models for the time-series scenario generally adopt one of two approaches: (i) a data-level fusion, or (ii) a feature-level fusion. In data-level fusion, the features for each day,  $\tilde{x}(t) \in \mathbb{R}^{H \times W \times C}$  are concatenated along the feature dimension into one input tensor,  $x(t) = [\tilde{x}(t-1), \dots, \tilde{x}(t-T)] \in \mathbb{R}^{H \times W \times CT}$ , after which they can

be processed in the same manner as single-day input (see Sec. 2 for problem notation). Therefore, we adopt our best-performing  $T = 1$  models from Sec. 6.1, and their hyperparameter settings, and evaluate them for data-level fusion. As a reference, we also include the *reported* results of the Res18-Unet [15] when it was applied for data-level fusion.

In this context, feature-level fusion implies that we use a shared encoder to first extract features (or embeddings) independently for each day of our input,  $\tilde{z}(t) = f_{\theta_{En}}(\tilde{x}(t))$  so that we have a collection of features,  $z(t) = \{\tilde{z}(t-i)\}_{i=1}^T$ , which are utilized as input into a subsequent model for joint processing (i.e., fusion). The current SOTA accuracy on WSTS, both for the time-series setting, and overall, was obtained with a UTAE model [14], as reported in [15]. Furthermore, the UTAE achieved superior accuracy despite having just 1.1M parameters - significantly fewer than many other models considered (e.g., the Res18-Unet has 14.3M). Therefore, we focus our modeling improvements on the UTAE from [15].

**Improvements to the UTAE** We develop two improved UTAE models, referred to as *UTAE* and *UTAE(Res18)*. We discuss the design of each model next.

*Our UTAE Model.* Our UTAE includes two major improvements over the UTAE[15]. The first improvement is to adopt all of the changes investigated for the single-day models from Sec. 6.1. Pursuant to this, following previous work convention, we did a joint search over the following hyperparameters using a single fold of the WSTS benchmark: pre-training (or not), learning rates ( $[1e-2, 1e-3, 1e-4, 1e-5]$ ), and the type of loss (Focal, BCE, Jaccard, and Dice loss). The second improvement is the introduction of relative positional encodings in the temporal fusion utilized by the UTAE, to replace the day-of-year embeddings (see Sec. 5 for review of topic, and notation). Specifically, instead of using positional encodings as in [14, 15] that are based upon the absolute day of the year, where  $\bar{t} \in [1, 365]$ , we propose to use a variant of relative positional encoding that indicates where in the daily sequence each feature is located, so that  $\bar{t} \in [1, \dots, T]$  for a T-day input. We hypothesize that the features (especially the fire mask) from the most recent day of the fire will be most important for making predictions, and therefore the relative position of each feature embedding in the sequence is much more important than its position in the year. Furthermore, it may be difficult for the models to infer relative positional information from absolute encodings, potentially undermining performance.

*Our UTAE(Res18) Model.* This model is obtained by making one additional improvement to our UTAE model. The encoder utilized in the UTAE[15] is relatively small (in terms of free parameters). Therefore, in similar fashion to our investigation in Sec. 6.1, we replace the existing UTAE’s encoder with a pre-trained ResNet-18.

Table 2. Mean test AP  $\pm$  standard deviation using vegetation features only (Veg), vegetation, land cover, topography and weather (Multi) and All features, when training with 1 and 5 input days. Models with citations represent accuracy reported on our benchmark from previous publications; all other models reported are developed in this work. Results style: **best**

Fusion Level	Model	Input days	Veg	Multi	All	# Params
Data	Res18-Unet[15]	1	0.328 $\pm$ 0.090	0.341 $\pm$ 0.085	0.341 $\pm$ 0.086	14.3M
	Res18-Unet	1	0.455 $\pm$ 0.090	<b>0.468 <math>\pm</math> 0.087</b>	<b>0.460 <math>\pm</math> 0.084</b>	14.3M
	Res50-Unet	1	<b>0.457 <math>\pm</math> 0.089</b>	0.459 $\pm$ 0.090	0.451 $\pm$ 0.093	32.5M
	SwinUnet	1	0.432 $\pm$ 0.088	0.437 $\pm$ 0.082	0.424 $\pm$ 0.090	27.2M
	Res18-Unet[15]	5	0.333 $\pm$ 0.079	0.344 $\pm$ 0.076	0.325 $\pm$ 0.108	14.4M
	Res18-Unet	5	<b>0.472 <math>\pm</math> 0.083</b>	<b>0.469 <math>\pm</math> 0.087</b>	<b>0.460 <math>\pm</math> 0.084</b>	14.4M
	SwinUnet	5	0.447 $\pm$ 0.087	0.453 $\pm$ 0.083	0.435 $\pm$ 0.079	27.3M
	UTAE[15]	5	0.372 $\pm$ 0.088	0.350 $\pm$ 0.113	0.321 $\pm$ 0.135	1.1M
	UTAE	5	0.452 $\pm$ 0.082	0.459 $\pm$ 0.088	0.433 $\pm$ 0.099	1.1M
Feature	UTAE(Res18)	5	<b>0.478 <math>\pm</math> 0.085</b>	<b>0.477 <math>\pm</math> 0.089</b>	<b>0.475 <math>\pm</math> 0.091</b>	14.6M

**Experimental Results** Tab. 2 reports the accuracy (in terms of AP) of our time-series models on the WSTS benchmark, categorized by the type of fusion performed: data-level or feature-level. Regarding data-level fusion, our *Res18-Unet* and *Swin-Unet* both substantially outperform the existing *Res18-Unet*[15] across all combinations of input features, with the *Res18-Unet* providing the best overall AP (AP=0.472, on Vegetation features). Regarding feature-level fusion, our two UTAE models (*UTAE* and *UTAE(Res18)*) substantially outperform the existing *UTAE*[15], which is the current SOTA model on WSTS, both for time-series input ( $T > 1$ ), and overall. Our *UTAE(Res18)* model achieves the highest overall performance for each combination of input features, across both single-day and time-series models. *In particular, our UTAE(Res18) achieves the highest overall AP with the Vegetation (Veg) feature subset, leading to a new overall SOTA performance on WSTS of AP=0.478.*

Notably, our results indicate that models receiving time-series input generally outperform those with single-day input. This is especially apparent when comparing data-level fusion models, such as *Res18-Unet* and *SwinUnet*, with their single-day counterparts, since they have few architectural differences. Most existing wildfire spread prediction in the literature has focused on the single-day input, however our findings here corroborate those from [15], and suggest that time-series modeling is a promising emerging modeling strategy.

Our results also provide evidence that each of our modeling improvements is beneficial. As discussed, our *UTAE* included several applicable improvements discussed for our single-day models in Sec. 6.1, as well as our improved temporal encodings described in this sub-section. We therefore conducted an ablation experiment, reported in Tab. 3, to demonstrate that our modified positional encodings pro-

Table 3. Test AP of UTAE trained on Vegetation features using the original Absolute positional encodings from [15], versus our proposed Relative positional encodings

Pos. Encodings	Absolute	Relative
UTAE	0.419 $\pm$ 0.101	<b>0.452 <math>\pm</math> 0.082</b>

vide additional benefits. To demonstrate that the pre-trained ResNet-18 encoder is beneficial, we can compare the performance of *UTAE(Res18)* and *UTAE* in Tab. 2: the pre-trained ResNet-18 is the only difference between these two models.

## 7. The WSTS+ Benchmark

Our results on the WSTS benchmark indicated that relatively simple models performed best, such as those based upon a ResNet-18, rather than models utilizing larger encoders (e.g., ResNet-50) or those utilizing attention (e.g., SwinUnet). This contrasts sharply with the broader vision literature where larger models tend to perform best, given sufficient quantities of training data. Therefore, we hypothesize that collecting more training data would facilitate the use of larger models, yielding superior modeling performance. To investigate this hypothesis, we expand the original WSTS benchmark by curating four additional years of historical wildfire data: 2016, 2017, 2022, and 2023. Our extended dataset, termed WSTS+, contains twice the number of years of historical wildfire data, expands the geographic diversity of the benchmark, and is – to our knowledge – the largest public benchmark for time-series next-day wildfire spread prediction. We visualize the geographic distribution of WSTS+ events in Fig. 4 and observe that it is mostly similar to WSTS around the Western United States, with some distinction in more eastern states. Tab. 4 sum-

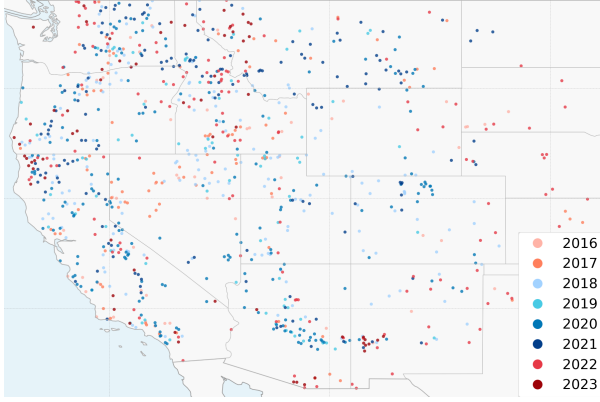


Figure 4. Geographic distribution of the fire events in each year of WSTS (blue) and WSTS+ (red)

marizes the differences between both datasets in terms of numbers of years, fire events, total images, and active fire pixels. Further collection details can be found in the Supplement.

Table 4. Comparison between the original WSTS dataset and our extension. We double the number of years and total images and drastically increase the number of fire events and active fire pixels.

Dataset	WSTS	WSTS+	Increase (%)
Years	4 (2018-2021)	8 (2016-2023)	+100
Fire Events	607	1,005	+65.6
Total Images	13,607	24,462	+79.8
Active Fire Px	1,878,679	2,638,537	+40.4

### 7.1. Benchmarking Models with WSTS+

As compared to WSTS, we propose a new scheme for evaluating models using WSTS+, which exploits its greater size to significantly reduce computational complexity compared to WSTS – thereby making the benchmark more accessible to researchers – while maintaining a similar level of real-world rigor. For WSTS+, we propose to divide the available data into four folds that each contain two consecutive years of historical wildfire data. We then evaluate models using four-fold cross-validation, where in each iteration, one fold of data is used for testing, one fold for validation, and two folds for training, as illustrated in Fig. 5. To ensure that the testing and validation sets have the same relative temporal distance to the training set, we always select them so that they are non-consecutive. This results in four-fold cross-validation instead of the twelve-fold cross-validation utilized in WSTS, making it much more accessible to researchers. At the same time, this approach doubles the quantity of data in the training and validation sets, ideally allowing researchers to train larger and more accurate models. Lastly, because two consecutive years of data are

1	(2016, 2017)	(2018, 2019)	(2020, 2021)	(2022, 2023)
2	(2016, 2017)	(2018, 2019)	(2020, 2021)	(2022, 2023)
3	(2016, 2017)	(2018, 2019)	(2020, 2021)	(2022, 2023)
4	(2016, 2017)	(2018, 2019)	(2020, 2021)	(2022, 2023)

Figure 5. New cross-validation folds used for WSTS+. Each pair of consecutive years is used as validation/testing once. Color code: blue: training, orange: validation, green: test

included in the test set, the benchmark still evaluates models under highly realistic and rigorous testing conditions,

Table 5. Mean test AP  $\pm$  standard deviation using vegetation features only (Veg), vegetation, land cover, topography and weather (Multi) and All features, when training on the WSTS+ dataset Results style: **best**

Model	Days	Veg	Multi	All
Res18-Unet	1	0.349 $\pm$ 0.109	0.351 $\pm$ 0.105	<b>0.351 <math>\pm</math> 0.122</b>
Res50-Unet	1	0.345 $\pm$ 0.096	0.353 $\pm$ 0.122	<b>0.351 <math>\pm</math> 0.122</b>
Res18-Unet-LTAE	5	<b>0.354 <math>\pm</math> 0.113</b>	<b>0.363 <math>\pm</math> 0.129</b>	0.350 $\pm$ 0.117

### 7.2. Experimental Results with WSTS+

Using our updated cross-validation scheme, we train our best  $T = 1$  models and our best  $T = 5$  model on WSTS+ and report the results in terms of mean average precision across all three feature sets in Tab. 5. We see that the performance rank-order of our three models is still similar on WSTS+ as compared to WSTS. However, the overall performance is significantly lower for these models on WSTS+ as compared to WSTS (by roughly 0.1 AP), and the differences in AP between the models are lower. These results seem to contradict our initial hypothesis that more training data would enable larger models and improve accuracy.

To investigate further, in Fig. 6, we measure the performance (in AP) across all eight years of data of our Res18-Unet model trained on WSTS or WSTS+, respectively. To estimate the WSTS+ models, we simply report the cross-validation test performance, stratified by year. We apply the same approach to the WSTS benchmark, obtaining performance metrics for 2018 to 2021. We select the best-performing Res18-Unet (as judged by its test fold error) and evaluate it to the four new years of WSTS data. The results in Fig. 6 indicate that, when viewed this way, the performances of the WSTS and WSTS+ models are very similar. In particular, models trained on each benchmark obtain similar AP on the original four years of the WSTS benchmark (the bolded years in Fig. 6), indicating that the two additional years of data that were available in each training fold of WSTS+ were not harmful; however, they were not helpful either, contradicting our initial hypothesis. Fig. 6 also reveals that the overall difficulty of the new years of data

- 2016, 2017, and 2022 in particular - are higher, as evidenced by the fact that all models perform much worse on those years, explaining why the overall AP on the WSTS+ is lower than WSTS.

Crucially, the results in Fig. 6 reveal substantial variance in model prediction accuracy across the eight years in WSTS+, regardless of which of our two models were utilized: WSTS or WSTS+. A similar pattern was observed on the WSTS benchmark [15], where the authors found similar variation in performance, which was stable across models trained with different years of training data. These findings could admit several explanations: label noise variations across different years, making some harder than others; each year may exhibit different feature distributions (i.e., domains shifts), or wildfire behavior may vary across years (i.e., concept shifts). Fig. 7 presents a UMAP visualization of the input features of WSTS years (in blue) and the new WSTS+ years (in red) at the deepest level of our best Res18-Unet encoder. While there is substantial overlap in the features obtained from each year of data, we also observe that many years seem to exhibit unique feature patterns. If some years exhibit especially unique feature distributions that are not present in any other years (or few other years) then it could contribute to low accuracy on those years.

**An Emerging Wildfire Modeling Challenge?** Our results suggest that naively combining historical wildfire data may not scale well across longer time frames (and perhaps space), if our goal is to train more accurate data-driven models. Yet substantial evidence from the broader computer vision literature indicates that developing larger training datasets is crucial to improve modeling. Therefore, an important emerging challenge for the wildfire modeling community may be to develop means of harmonizing, and/or otherwise effectively utilizing diverse historical wildfire data to train data-driven models. We hypothesize that developing such methods may be key to obtaining better accuracy on the WSTS+ benchmark, and therefore that the benchmark will be a useful resource for developing solutions.

## 8. Conclusion

In this work, we focus on the problem of next-day wildfire spread prediction, where we are provided with current and/or historical information about a particular wildfire, and then tasked with predicting its spatial extent on the following day. We introduce a variety of modeling improvements in two scenarios: single-day ( $T = 1$ ) and time-series ( $T > 1$ ) input scenarios. Our results show that these improvements lead to substantial increases in accuracy over the existing state-of-the-art, as demonstrated on the WildfireSpreadTS (WSTS) benchmark [15], resulting in signif-

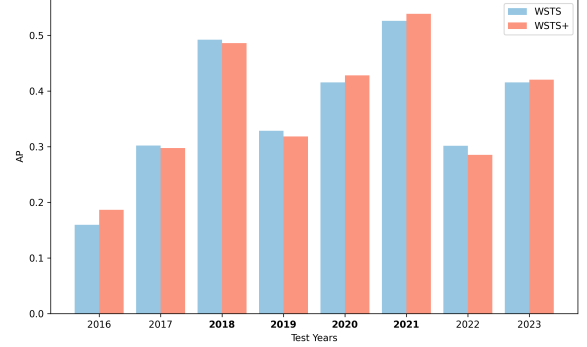


Figure 6. Performance breakdown by test year. Blue bars represent models trained on the original WSTS data, while red bars represent those trained on WSTS+. The bolded x-axis ticks highlight original test years from WSTS.

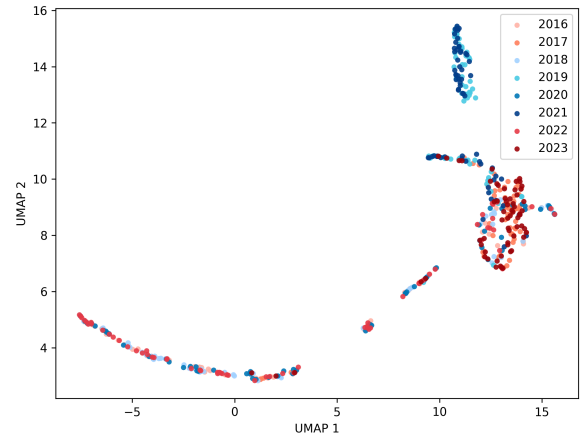


Figure 7. UMAP visualization of the inputs features across years. Each point represents the encoded features at the deepest layer of our best Res18-Unet encoder, with blue indicating original WSTS year and red newly added years in WSTS+.

icant increases in the current state-of-the-art accuracy on WSTS. Lastly, we introduce WSTS+, an extended benchmark for next-day wildfire spread, constructed by doubling the number of years of historical wildfire events in WSTS and resulting, to our knowledge, in the largest public benchmark for *time-series* next-day wildfire spread prediction. The WSTS+ also reveals an emerging challenge for the wildfire modeling community: historical data heterogeneity. We hypothesize that developing models that can handle more heterogeneity (e.g., domain or concept shifts) across data may be key to obtaining better accuracy on the WSTS+ benchmark, and therefore that the WSTS+ benchmark will be a useful resource for developing such solutions.

## References

- [1] Martin E Alexander and Miguel G Cruz. Evaluating a model for predicting active crown fire rate of spread using wildfire



- observations. *Canadian Journal of Forest Research*, 36(11): 3015–3028, 2006. 1
- [2] Tomàs Artés, Duarte Oom, Daniele De Rigo, Tracy Houston Durrant, Pieralberto Maianti, Giorgio Libertà, and Jesús San-Miguel-Ayanz. A global wildfire dataset for the analysis of fire regimes and fire behaviour. *Scientific data*, 6(1):296, 2019. 2
- [3] Andrew Bolt, Carolyn Huston, Petra Kuhnert, Joel Janek Dabrowski, James Hilton, and Conrad Sanderson. A spatio-temporal neural network forecasting approach for emulation of firefront models. In *2022 Signal Processing: Algorithms, Architectures, Arrangements, and Applications (SPA)*, pages 110–115. IEEE, 2022. 2
- [4] Karol Bot and José G Borges. A systematic review of applications of machine learning techniques for wildfire management decision support. *Inventions*, 7(1):15, 2022. 1
- [5] John Burge, Matthew R Bonanni, R Lily Hu, and Matthias Ihme. Recurrent convolutional deep neural networks for modeling time-resolved wildfire spread behavior. *Fire Technology*, 59(6):3327–3354, 2023. 2
- [6] Hu Cao, Yueyue Wang, Joy Chen, Dongsheng Jiang, Xiaopeng Zhang, Qi Tian, and Manning Wang. Swin-unet: Unet-like pure transformer for medical image segmentation. In *European conference on computer vision*, pages 205–218. Springer, 2022. 3, 4, 1
- [7] Jieneng Chen, Yongyi Lu, Qihang Yu, Xiangde Luo, Ehsan Adeli, Yan Wang, Le Lu, Alan L Yuille, and Yuyin Zhou. Transunet: Transformers make strong encoders for medical image segmentation. *arXiv preprint arXiv:2102.04306*, 2021. 1
- [8] Khaled Chetehouna, Eddy El Tabach, Loubna Bouazaoui, and Nicolas Gascoin. Predicting the flame characteristics and rate of spread in fires propagating in a bed of pinus pinaster using artificial neural networks. *Process Safety and Environmental Protection*, 98:50–56, 2015. 1
- [9] Tom Eelbode, Jeroen Bertels, Maxim Berman, Dirk Vandermeulen, Frederik Maes, Raf Bisschops, and Matthew B Blaschko. Optimization for medical image segmentation: theory and practice when evaluating with dice score or jaccard index. *IEEE transactions on medical imaging*, 39(11): 3679–3690, 2020. 4
- [10] Mark A. Finney. *FARSITE: Fire Area Simulator-model development and evaluation*. 1998. 1
- [11] Mark A Finney. An overview of flammap fire modeling capabilities. In *In: Andrews, Patricia L.; Butler, Bret W., comps. 2006. Fuels Management-How to Measure Success: Conference Proceedings. 28-30 March 2006; Portland, OR. Proceedings RMRS-P-41. Fort Collins, CO: US Department of Agriculture, Forest Service, Rocky Mountain Research Station. p. 213-220, 2006*. 1
- [12] Jack Fitzgerald, Ethan Seefried, James E Yost, Sangmi Pallickara, and Nathaniel Blanchard. Paying attention to wildfire: Using u-net with attention blocks on multimodal data for next day prediction. In *Proceedings of the 25th International Conference on Multimodal Interaction*, pages 470–480, 2023. 3, 4
- [13] Vivien Sainte Fare Garnot and Loic Landrieu. Lightweight temporal self-attention for classifying satellite images time series. In *Advanced Analytics and Learning on Temporal Data: 5th ECML PKDD Workshop, AALTD 2020, Ghent, Belgium, September 18, 2020, Revised Selected Papers 6*, pages 171–181. Springer, 2020. 3
- [14] Vivien Sainte Fare Garnot and Loic Landrieu. Panoptic segmentation of satellite image time series with convolutional temporal attention networks. In *Proceedings of the IEEE/CVF International Conference on Computer Vision*, pages 4872–4881, 2021. 2, 3, 5, 1
- [15] Sebastian Gerard, Yu Zhao, and Josephine Sullivan. Wildfirespreads: A dataset of multi-modal time series for wildfire spread prediction. *Advances in Neural Information Processing Systems*, 36:74515–74529, 2023. 2, 3, 4, 5, 6, 8, 1
- [16] Rohit Ghosh, Jishnu Adhikary, and Rezki Chemlal. Fire spread modeling using probabilistic cellular automata. In *Asian Symposium on Cellular Automata Technology*, pages 45–55. Springer, 2024. 3
- [17] Luis Giglio, Chris Justice, Luigi Boschetti, and David Roy. Modis/terra+ aqua burned area monthly 13 global 500m sin grid v061. *NASA EOSDIS Land Process. DAAC*, 2021. 2
- [18] Julia Gottfriedsen, Johanna Strebl, Max Berrendorf, Martin Langer, and Volker Tresp. Firesight: Short-term fire hazard prediction based on active fire remote sensing data. 2
- [19] Kaiming He, Xiangyu Zhang, Shaoqing Ren, and Jian Sun. Deep residual learning for image recognition. In *Proceedings of the IEEE conference on computer vision and pattern recognition*, pages 770–778, 2016. 3, 4
- [20] Fantine Huot, R Lily Hu, Nita Goyal, Tharun Sankar, Matthias Ihme, and Yi-Fan Chen. Next day wildfire spread: A machine learning dataset to predict wildfire spreading from remote-sensing data. *IEEE Transactions on Geoscience and Remote Sensing*, 60:1–13, 2022. 2, 3
- [21] Vladimir Iglovikov and Alexey Shvets. Ternaunet: U-net with vgg11 encoder pre-trained on imagenet for image segmentation. *arXiv preprint arXiv:1801.05746*, 2018. 3
- [22] Sadeqh Khanmohammadi, Mehrdad Arashpour, Emadaldin Mohammadi Golafshani, Miguel G Cruz, Abbas Rajabifard, and Yu Bai. Prediction of wildfire rate of spread in grasslands using machine learning methods. *Environmental Modelling & Software*, 156:105507, 2022. 1
- [23] Spyros Kondylatos, Ioannis Prapas, Michele Ronco, Ioannis Papoutsis, Gustau Camps-Valls, María Piles, Miguel-Ángel Fernández-Torres, and Nuno Carvalhais. Wildfire danger prediction and understanding with deep learning. *Geophysical Research Letters*, 49(17):e2022GL099368, 2022. 2
- [24] Bronte Sihan Li and Ryan Rad. Wildfire spread prediction in north america using satellite imagery and vision transformer. In *2024 IEEE Conference on Artificial Intelligence (CAI)*, pages 1536–1541. IEEE, 2024. 3, 4
- [25] Jiangyun Li, Yuanxiu Cai, Qing Li, Mingyin Kou, and Tianxiang Zhang. A review of remote sensing image segmentation by deep learning methods. *International Journal of Digital Earth*, 17(1):2328827, 2024. 3
- [26] Yanzhi Li, Keqiu Li, LI GUOHUI, Chanqing Ji, Lubo Wang, Die Zuo, Qing Guo, Feng Zhang, Manyu Wang, Di Lin, et al. Sim2real-fire: A multi-modal simulation dataset for forecast and backtracking of real-world forest fire. In *The Thirty-*

- eight Conference on Neural Information Processing Systems Datasets and Benchmarks Track. 3
- [27] Tsung-Yi Lin, Priya Goyal, Ross Girshick, Kaiming He, and Piotr Dollár. Focal loss for dense object detection. In *Proceedings of the IEEE international conference on computer vision*, pages 2980–2988, 2017. 4
  - [28] Shuwen Liu, Lin Cao, Chuanying Lin, Yuxuan Dai, Xingdong Li, Sanping Li, Shufa Sun, and Dandan Li. Fire spread prediction model based on multi-scale convolutional neural network. *Multimedia Tools and Applications*, pages 1–22, 2024. 2
  - [29] Ze Liu, Yutong Lin, Yue Cao, Han Hu, Yixuan Wei, Zheng Zhang, Stephen Lin, and Baining Guo. Swin transformer: Hierarchical vision transformer using shifted windows. In *Proceedings of the IEEE/CVF international conference on computer vision*, pages 10012–10022, 2021. 1
  - [30] Mohammad Marjani, Masoud Mahdianpari, and Fariba Mohammadimanesh. Cnn-bilstm: A novel deep learning model for near-real-time daily wildfire spread prediction. *Remote Sensing*, 16(8):1467, 2024. 2
  - [31] Dimitrios Michail, Lefki-Ioanna Panagiotou, Charalampos Davalas, Ioannis Prapas, Spyros Kondylatos, Nikolaos Ioannis Bountos, and Ioannis Papoutsis. Seasonal fire prediction using spatio-temporal deep neural networks. *arXiv preprint arXiv:2404.06437*, 2024. 2
  - [32] MTBS Project, USDA Forest Service/U.S. Geological Survey. MTBS Data Access: Fire Level Geospatial Data, 2017. Last revised. 2
  - [33] Ozan Oktay. Attention u-net: Learning where to look for the pancreas. *arXiv preprint arXiv:1804.03999*, 2018. 1
  - [34] Ioannis Prapas, Akanksha Ahuja, Spyros Kondylatos, Ilektra Karasante, Eleanna Panagiotou, Lazaro Alonso, Charalampos Davalas, Dimitrios Michail, Nuno Carvalhais, and Ioannis Papoutsis. Deep learning for global wildfire forecasting. *arXiv preprint arXiv:2211.00534*, 2022. 2
  - [35] Olaf Ronneberger, Philipp Fischer, and Thomas Brox. U-net: Convolutional networks for biomedical image segmentation. In *Medical image computing and computer-assisted intervention—MICCAI 2015: 18th international conference, Munich, Germany, October 5-9, 2015, proceedings, part III 18*, pages 234–241. Springer, 2015. 3, 1
  - [36] William L Ross. Being the fire: A cnn-based reinforcement learning method to learn how fires behave beyond the limits of physics-based empirical models. In *NeurIPS 2021 Workshop on Tackling Climate Change with Machine Learning*, 2021. 3
  - [37] Kamen Shah and Maria Pantoja. Wildfire spread prediction using attention mechanisms in u-net. In *2023 3rd International Conference on Electrical, Computer, Communications and Mechatronics Engineering (ICECCME)*, pages 1–6. IEEE, 2023. 2, 3, 4
  - [38] Douglas Thomas, David Butry, Stanley Gilbert, David Webb, Juan Fung, et al. The costs and losses of wildfires. *NIST special publication*, 1215(11):1–72, 2017. 1
  - [39] Hongtao Xiao, Yingfang Zhu, Yurong Sun, Gui Zhang, and Zhiwei Gong. Wildfire spread prediction using attention mechanisms in u2-net. *Forests*, 15(10):1711, 2024. 3, 4
  - [40] Zhengsen Xu, Jonathan Li, Sibbo Cheng, Xue Rui, Yu Zhao, Hongjie He, and Linlin Xu. Wildfire risk prediction: A review. *arXiv preprint arXiv:2405.01607*, 2024. 3
  - [41] Zongwei Zhou, Md Mahfuzur Rahman Siddiquee, Nima Tajbakhsh, and Jianming Liang. Unet++: A nested u-net architecture for medical image segmentation. In *Deep Learning in Medical Image Analysis and Multimodal Learning for Clinical Decision Support: 4th International Workshop, DLMIA 2018, and 8th International Workshop, ML-CDS 2018, Held in Conjunction with MICCAI 2018, Granada, Spain, September 20, 2018, Proceedings 4*, pages 3–11. Springer, 2018. 2
  - [42] Yufei Zou, Mojtaba Sadeghi, Yaling Liu, Alexandra Puchko, Son Le, Yang Chen, Niels Andela, and Pierre Gentine. Attention-based wildland fire spread modeling using fire-tracking satellite observations. *Fire*, 6(8):289, 2023. 4

# Advancing Time Series Wildfire Spread Prediction: Modeling Improvements and the WSTS+ Benchmark

## Supplementary Material

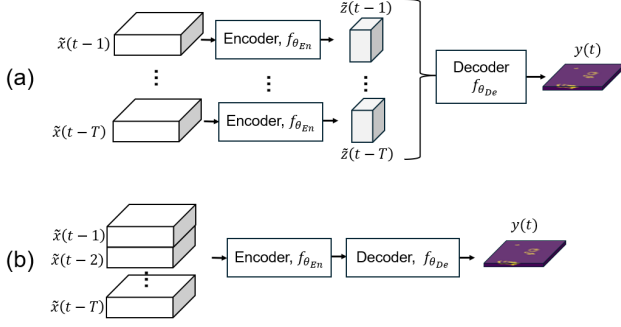


Figure 8. Illustration of (a) feature-level fusion, and (b) data-level fusion as we define it here. Further description is provided in the main text, and mathematical notation is described in Sec. 2

## 9. Experimental Details

**SwinUnet** SwinUnet [6] is a pure transformer-based Unet-shaped model that was first proposed for medical imagery segmentation. The model replaces the convolution blocks of the Unet with Swin Transformer blocks [29], including them throughout the encoder, bottleneck, and decoder. They also rely on patch merging and patch expansion layers in the encoder and decoder, respectively, to downsample the input features and then upsample the extracted features and produce the segmentation mask. Finally, they preserve skip connections to concatenate shallow and deep features. The SwinUnet outperformed the Unet [35], ViT [7], Att-Unet [33], and TransUnet [7] on two medical benchmark datasets. Its state-of-the-art performance, ability to learn both global and long-range dependencies, and use of the more efficient Swin blocks make it a good candidate for our task. Since the model was developed for RGB images, we modify the `in_chans` parameter to take in the number of channels of our multi-modal inputs (Veg: 7, Multi: 33, All: 40) instead of 3.

**Model pre-training** To evaluate the effect of pre-training on the SwinUnet model, we load the `swin-tiny-patch4-window7-224` weights from HuggingFace onto each of our Swin blocks. These weights correspond to a Swin Transformer trained on ImageNet at 224x224 resolution. We zero-pad our input images (128x128) to match the expected input dimensions and benefit from the pre-trained weights. As for the Unet models, we follow [15] and use the `segmentation_models_pytorch` implementation,

Table 6. Proposed cross-validation splits for WSTS+

Fold	Train	Val	Test
1	(2016, 2017, 2020, 2021)	(2018, 2019)	(2022, 2023)
2	(2018, 2019, 2022, 2023)	(2016, 2017)	(2016, 2017)
3	(2016, 2017, 2020, 2021)	(2022, 2023)	(2018, 2019)
4	(2018, 2019, 2022, 2023)	(2020, 2021)	(2016, 2017)

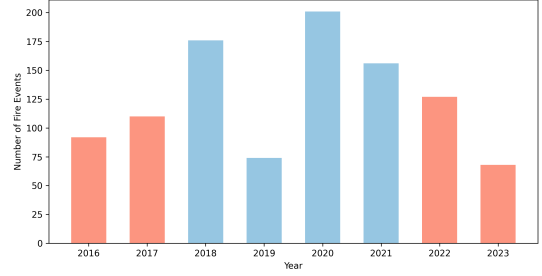


Figure 9. Distribution of fire events per year

and set `encoder_weights` to `imagenet`, which loads a model with ImageNet pre-trained weights. Finally, the UTAE pre-training uses the PASTIS weights, released with the original paper [14]. We use the 4th fold checkpoint, as it was the one with the highest performance.

**Training details** To train our models, we adopt the implementations shared by [15], which can be found in [this GitHub repository](#). The implementation relies on PyTorch Lightning for model creation, training, and testing and Weights & Biases for model logging and metric visualization. All our models use a fixed batch size of 64, the AdamW optimizer, and a fixed optimized learning rate, as described in Sec. 6. Also following [15], we train our models for 10,000 iterations. Increasing the number of iterations to 15,000 and 20,000 did not yield any notable increases in performance. For all runs in Tab. 2, we report the mean test AP averaged over the 12 folds, and the standard deviation. During the hyperparameter search, we only use a single data fold (`id = 2`), train for 50 epochs, and pick the combination that yields the highest validation AP.

## 10. WSTS+ Details

To ensure our added wildfire events are most similar to the original ones, we follow the exact same collection procedure in [15]. Namely, we only collect wildfires that are

larger than  $10 \text{ km}^2$ , and use the GlobFire dataset [2] to identify wildfire events in the United States for 2016 and 2017. However, given GlobFire’s temporal availability ends at 2021, we use MTBS Burned Areas Boundaries Dataset [32] to identify wildfires in 2022 and 2023.

The main differences between both datasets used for fire event identification are that GlobFire relies on MODIS [17] as a data source, which has a resolution of 500 meters, while MTBS uses Landsat imagery, which has 30 meter resolution. This should not impact the dataset homogeneity, as these datasets are only used to find wildfire coordinates, therefore having higher resolution is neither advantageous nor disadvantageous. Furthermore, GlobFire returns burned area maps with start and end dates, while MTBS returns fire perimeters with start dates only. This also has little effect, since we only use the centroid coordinate for both area maps and perimeters to download the fire masks. To account for the lack of fire end dates in MTBS, we collect 30 days of samples after the start date, with an additionnal buffer of 4 days before and after the fire events, similar to [15].